

ORIGINAL ARTICLE

Effects of heating rate, quartz particle size, viscosity, and form of glass additives on high-level waste melter feed volume expansion

SeungMin Lee¹ | Bradley J. VanderVeer¹ | Pavel Hрма¹ | Zachary J. Hilliard¹ | Jayven S. Heilman-Moore¹ | Charles C. Bonham¹ | Richard Pokorny² | Derek R. Dixon¹ | Michael J. Schweiger¹ | Albert A. Kruger³

¹Pacific Northwest National Laboratory, Richland, Washington

²Laboratory of Inorganic Materials, Joint Workplace of the University of Chemistry and Technology and the Institute of Rock Structure and Mechanics of the ASCR, Prague 8, Czech Republic

³U.S. Department of Energy, Office of River Protection, Richland, Washington

Correspondence

Bradley J. VanderVeer, Pacific Northwest National Laboratory, Richland, WA.
Email: seungmin.lee@pnnl.gov

Abstract

Nuclear waste can be vitrified by mixing it with glass-forming and -modifying additives. The resulting feed is charged into an electric glass melter. To comprehend melting behavior of a high-alumina melter feed, we monitored the volume expansion of pellets in response to heating at different heating rates. The feeds were prepared with different particle sizes of quartz (the major additive component) and with varied silica-to-fluxes ratio to investigate the glass melt viscosity effects. Also, we used additional melter feeds with additives premelted into glass frit. The volume of pellets was nearly constant at temperatures <600°C. After a short period of volume shrinkage at ~600°C-700°C, foam generation produced massive volume expansion. The low heat conductivity of foam hinders the transfer of heat from molten glass to the reacting feed. The extent of foaming increased with faster heating and higher melt viscosity, and decreased with increasing size of quartz particles and fritting of the additives. Volume expansion data are needed for the mathematical modeling of the cold cap.

KEYWORDS

cold cap, frit, glass-forming and -modifying chemicals, heating rate, high-level waste, quartz particle size, viscosity

1 | INTRODUCTION

Nuclear waste can be vitrified by mixing it with glass-forming and -modifying additives to produce melter feed in the form of slurry or calcine, which is subsequently charged into an electric melter. In a joule-heated melter, the feed is converted into glass. The conversion occurs in the cold cap, a reacting mass that floats on the surface of molten glass.¹⁻⁴ Together with the waste loading in the glass, the rate of conversion (the rate of melting) is a major factor in the glass production efficiency.⁵⁻⁹ It is influenced by the mineralogical form of the glass additives, the particle size of solids, the loading and type of waste, and the

melter feed rheology.^{5,6} The rate of melting is adversely impacted by the thermally insulating effect of foam that forms between the main body of the cold cap and the melt pool.

To understand the behavior of melter feed in the cold cap and to find trends relevant for the melting rate—in particular foaming—this study is focused on the effects of heating rate, quartz particle size, melt viscosity, and the form of the glass additives on melter feed volume expansion. These influential effects have not been addressed by previous studies. Accordingly, four series of experiments were performed: a heating rate series (heating the feed sample at 5 to 30 K/min), a quartz particle size series

(using narrow fractions from 5 to 250 μm), a melt viscosity series (from 1.5 to 9.5 Pa·s at 1150°C), and a glass-forming additive series (using frit or loose chemicals). The heating rate series was motivated by the fact that the rate of melting and the rate of heating are intimately correlated.^{3,4} The next two series were motivated by the well-known facts that the quartz particle size and the melt viscosity are major factors in melting behavior of commercial glass batches⁵ as well as nuclear waste melter feeds.⁵⁻⁷ Finally, the effect of fritting glass additives was included in this study. Frit is believed to stabilize the melting process and enhance the rate of melting.^{6,10} Frit is commonly used by waste glass producers in the United States (Savannah River Site),^{8,9} France, Germany, and other countries.¹⁰⁻¹⁴ The graphs of volume expansion vs temperature provide data for further analyses, especially with respect to the bulk density and the heat conductivity of the reacting feeds. Such data are indispensable for mathematical modeling of feed-to-glass conversion in the cold cap.^{3-5,15-17}

2 | EXPERIMENTAL PROCEDURE

2.1 | Feeds

The heating rate series, quartz particle size series, and viscosity series were performed with the A19 feed,^{18,19} a simplified version of melter feed designed by the Vitreous State Laboratory for high-alumina nuclear waste.²⁰ For the viscosity series, the glass composition was varied as described below [Section II(3)]. For the frit vs glass-forming and -modifying chemicals (GFMC) series, two melter feeds, high boron-low alkali (Feed I) and low boron-high alkali (Feed II), were obtained from Savannah River National Laboratory (SRNL).^{6,21} Table 1 displays the chemical compounds and their amounts added to make 1 kg glass for the feeds used. These feeds were designed for glasses of compositions given in Table 2.

The A19 feeds (the original feed, Table 1, and its modified versions to vary viscosity) were prepared following the procedure described in our previous works.^{19,22} First, all chemicals except quartz were mixed with water to prepare a slurry that was subsequently dried in an oven at 105°C overnight and milled to powder. To prepare the feed samples for testing, the powder was manually mixed with an adequate amount of quartz specified in Table 1.

2.2 | Quartz particle size fractions

Quartz particle size fractions (Table 3) were prepared from SIL-CO-SIL 250 (99.9% SiO₂, U.S. Silica, Frederick, MD, USA) by sieving. The fractions were washed in deionized water and then in ethanol using an ultrasonic cleaner and then dried in the oven at 90°C for 1 hour. For the feed

TABLE 1 Compositions of A19-original and SRNL batches in g to make 1 kg glass

	A19-original	Feed I	Feed II
Al(OH) ₃	371.79	117.50	152.75
B(OH) ₃	341.59	338.91	154.05
BaO		0.49	0.59
Bi ₂ O ₃	11.67		
CaO	10.87	3.96	5.09
Cr ₂ O ₃	6.20	0.83	1.00
CuO		0.40	0.60
Fe(NO ₃) ₃		319.69	365.36
Fe(OH) ₃	74.38		
Fe(H ₂ PO ₂) ₃	12.51		
KNO ₃		0.57	0.97
Li ₂ CO ₃	89.22	7.68	
Mg(OH) ₂		4.00	4.80
KMnO ₄		68.70	77.86
NaOH	19.87	162.00	226.80
Ni(NO ₃) ₂ (H ₂ O) ₆		43.20	56.16
Ni(OH) ₂	5.03		
SiO ₂	221.45	381.37	381.37
TiO ₂		0.31	0.31
ZnO		0.51	0.51
ZrO ₂		0.48	0.48
Zr(OH) ₄	5.53		
NaAlO ₂		7.50	7.50
Mg(NO ₃) ₂		8.00	8.00
CaCO ₃		1.92	1.92
CaSiO ₃	97.07		
Na ₂ C ₂ O ₄	1.26	2.22	2.22
Na ₂ CO ₃	106.57	24.15	24.15
Na ₂ SO ₄	3.60	5.15	6.44
NaPO ₄		1.59	1.59
NaF	15.00	0.27	0.27
NaCl		0.97	0.97
NaNO ₂	3.48	30.40	30.40
NaNO ₃	12.40	27.80	27.80
PbO	4.17	0.07	0.07
Ce(OH) ₃		0.90	0.90
Total (g)	1413.66	1561.54	1540.92

containing ≤ 5 μm quartz particles, MIN-U-SIL 5 (99.9% SiO₂, U.S. Silica) was used.

The quartz particle size fraction of 63-75 μm was used for the viscosity series. The heating rate series was carried out with as-received (unsieved) SIL-CO-SIL 75 (99.9% SiO₂, U.S. Silica).

TABLE 2 Compositions of A19-original and SRNL glasses in mass fractions

	A19-original	Glass I	Glass II
Al ₂ O ₃	0.2420	0.0895	0.1000
B ₂ O ₃	0.1919	0.2000	0.0862
BaO	0.0000	0.0005	0.0006
Bi ₂ O ₃	0.0116	0.0000	0.0000
CaO	0.0559	0.0055	0.0061
Cr ₂ O ₃	0.0053	0.0009	0.0010
CuO	0.0000	0.0005	0.0006
F	0.0067	0.0000	0.0000
Fe ₂ O ₃	0.0596	0.1069	0.1194
K ₂ O	0.0000	0.0013	0.0015
Li ₂ O	0.0357	0.0031	0.0000
MgO	0.0000	0.0050	0.0055
MnO	0.0000	0.0309	0.0346
Na ₂ O	0.0961	0.1383	0.2264
NiO	0.0040	0.0132	0.0147
P ₂ O ₅	0.0106	0.0008	0.0009
PbO	0.0041	0.0000	0.0000
SO ₃	0.0020	0.0031	0.0035
SiO ₂	0.2704	0.3836	0.3801
SnO ₂	0.0000	0.0003	0.0003
TiO ₂	0.0000	0.0003	0.0003
ZnO	0.0000	0.0005	0.0005
ZrO ₂	0.0040	0.0005	0.0005

TABLE 3 Quartz particle size fractions

Source	Range (μm)
SIL-CO-SIL 250	106-250
	90-106
	75-90
	63-75
	45-63
	25-45
	≤25
SIL-CO-SIL 75	≤75
MIN-U-SIL 5	≤5

2.3 | Viscosity variation

For the viscosity series, the feeds were formulated to make five glasses of estimated viscosities varying from 1.5 to 9.5 Pa·s at 1150°C (Table 4). Melt viscosity variation was accomplished by changing the SiO₂/

(B₂O₃ + Na₂O + Li₂O) ratio, where the chemical formulas signify the mass fractions of the oxide components in the glass.¹⁹ The mass fractions of all components other than SiO₂, B₂O₃, Na₂O, and Li₂O remained the same as in the A19 original.^{19,20} The mass fractions of B₂O₃, Na₂O, and Li₂O were in the same proportions as in the A19 original (Table 1; see Ref. [19] for the full list of compositions).

For the viscosity-glass composition relationship, we used the formula²³⁻²⁷

$$\ln \eta = A + \frac{1}{T} \sum_{i=1}^N B_i x_i \quad (1)$$

where η is viscosity, A is a constant coefficient, B_i is the i th component's partial specific activation energy, x_i is the i th component's mass fraction, T is the absolute temperature, and N is the number of components. The values of coefficients used were $A = -11.19$ (to obtain η in Pa·s), and $B_i = 3.00 \times 10^4$ K for SiO₂, 0.32×10^4 K for B₂O₃, -0.04×10^4 K for Na₂O, and -3.91×10^4 K for Li₂O.²³

Viscosity was measured with a rotating spindle viscometer (Brookfield RVDV-III, Middleboro, MA, USA). Glasses were prepared from dry chemicals, melted in a covered platinum crucible for 1 hour at 1150°C, milled to powder, and remelted at the same temperature. Figure 1 and Table 4 compare measured and estimated data, and indicate reasonable agreement.

2.4 | Frits and glass-forming chemicals

Feeds I and II (Table 1) were prepared by blending the waste stimulant with H₃BO₃, SiO₂, Na₂CO₃, and Li₂CO₃, either as loose chemicals or as premelted frit. To make frit, the chemicals were melted at 1150°C for 30 minute in a platinum crucible. The melt was poured onto a stainless steel plate, cooled in air, ground, and remelted under the same conditions. The glass was then ground and sieved to a particle size of 74-177 μm. The feeds as received from SRNL, both those made with frits and with loose chemicals, were dried in the oven at 100°C overnight and passed through a 10-mesh screen.

(5) | Pellet preparation, heat treatment, and pellet volume measurement

Dry feeds were prepared as described in Sections II(1) to II (4). Feeds were pressed into 1.5-g pellets at 168 MPa for 90 seconds. Pellets were circular disks ~13 mm in diameter and ~6 mm thick.

For the heat treatment, a pellet was placed on a circular alumina plate 33 mm in diameter and 2.5 mm thick that was placed in the furnace. The furnace was heated from room temperature to 1100°C at 10 K/min (5, 10, 20, and 30 K/min for heating rate series). The profile of the pellet

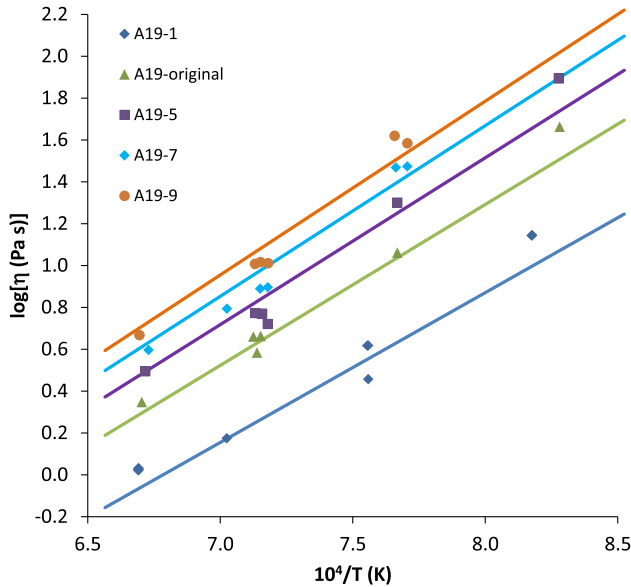


FIGURE 1 Measured (data points) and estimated (solid lines) viscosities of glasses A19-1 through A19-9. [Color figure can be viewed at wileyonlinelibrary.com]

was monitored with a camera through a quartz-glass window in the side wall of the furnace. Figure 2 shows photos of pellets at various temperatures. Each picture of a pellet was processed with Photoshop[®] software and the MATLAB[®] program to determine the pellet volume by numerical integration.²⁸ Up to three pellets were used to get statistically significant data. A similar method for visual observation of feed-to-glass conversion was reported in Ref. [29].

3 | RESULTS

Figures 3-5 show the normalized volume of A19 feeds vs temperature with the heating rates, quartz particle sizes, and viscosities as parameters. The normalized volume is defined as $V=V_T/V_0$, where V_T is the pellet volume at temperature T , and V_0 is the initial pellet volume. Figure 6 compares normalized volume of the pellets made from two

SRNL feeds, each with either frit or GFMC. In Figures 3-6, dots indicate measured data points and lines show calculated moving averages.

Figures 7-9 display normalized volume (V) and temperature (T) at the foam onset (the minima in Figures 3-5) and maximum foam (maxima in Figures 3-5) as functions of the heating rate (β), quartz particle size (d), and the value of melt viscosity (η) at 1150°C; subscripts min and max denote the foam onset and the maximum sample volume, respectively. The heating rate and viscosity series followed linear trends. Exponential functions were fitted (using the least-squares method) to data of the quartz particle size series.

Because of the shift of the reaction rate peaks to higher temperatures at higher rates of heating,³⁰ one would expect a similar response of feed foaming. As Figures 3 and 7 show, this was indeed the case. When heated faster, the feed generated more foam that started a lower temperature and culminated at a higher temperature.

As seen in Figures 4 and 8, feeds with small particles of silica generated more foam that started at lower temperatures. As described in earlier studies,^{17,26-28} this is a result of fast dissolution of fine quartz particles during early batch reactions with molten salts, while coarser quartz particles dissolve mostly in a continuous glass phase via diffusion. The volume at the foam onset and the temperature at which foam culminated changed little with the particle size.

As Figures 5 and 9 demonstrate, higher viscosity gives rise to a higher volume expansion. In addition, the foam onset and maximum foam temperatures increase linearly with the viscosity.

4 | DISCUSSION

The dry-feed pellet test, or the feed expansion test, employed in this study was designed to measure feed volume in response to increasing temperature. The pellet can be heated following the temperature history that the feed experiences within the cold cap. In this study, we used a

TABLE 4 Ratio of SiO₂, activation energy (B), and viscosity (η) of modified A19 feed series

	A19-original	A19-1	A19-5	A19-7	A19-9
SiO ₂ /(Li ₂ O + B ₂ O ₃ + Na ₂ O)	0.84	0.65	0.95	1.05	1.12
B (10 ⁴ K)					
Estimated	1.771	1.649	1.835	1.879	1.913
Measured	1.775	1.666	1.844	1.872	1.925
η (Pa·s) at 1150°C					
Estimated	3.49	1.49	5.49	7.49	9.49
Measured	3.56	1.79	5.36	6.21	9.00

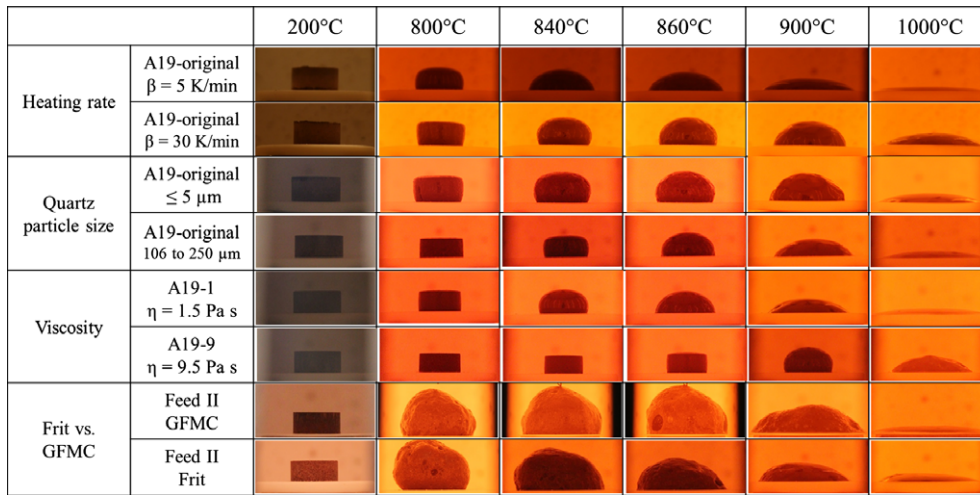


FIGURE 2 Profiles of pellets: A19-original feeds heated 5 and 30 K/min, A19-original feeds with small ($\leq 5 \mu\text{m}$) and large (106–250 μm) quartz particles, modified A19 feeds with viscosities 1.5 and 9.5 Pa·s, and Feed II with glass-forming and -modifying chemicals (GFMC) and frit. [Color figure can be viewed at [wileyonlinelibrary.com](#)]

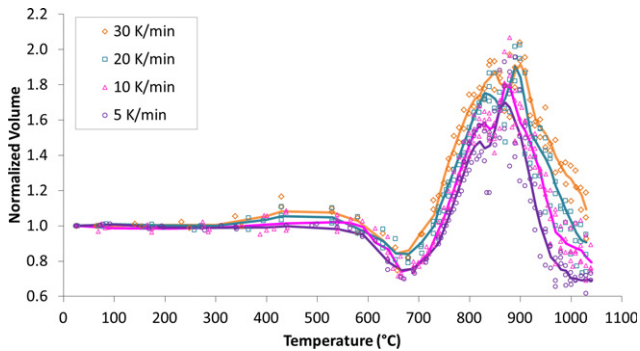


FIGURE 3 Normalized volume of A19-original feeds (with quartz particles $\leq 75 \mu\text{m}$) subjected to heating rates from 5 to 30 K/min vs temperature. [Color figure can be viewed at [wileyonlinelibrary.com](#)]

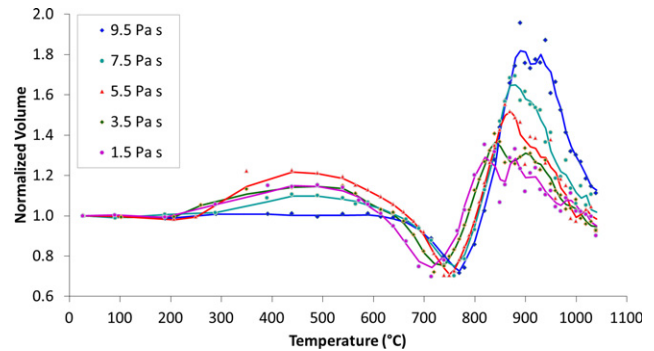


FIGURE 5 Normalized volume of A19 feeds with different glass viscosities vs temperature: the feeds contained 63–75 μm quartz particles and pellets were heated at 10 K/min. [Color figure can be viewed at [wileyonlinelibrary.com](#)]

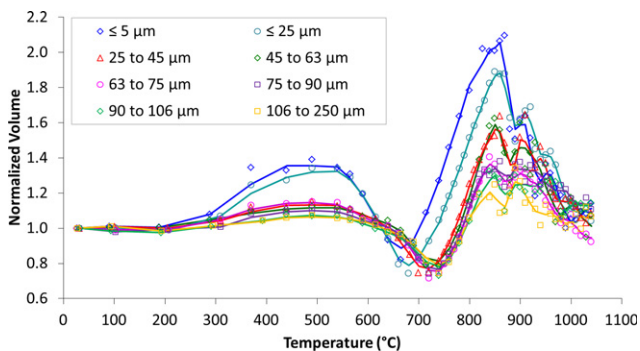


FIGURE 4 Normalized volume of A19-original feeds with different quartz particle sizes vs temperature; pellets were heated at 10 K/min. [Color figure can be viewed at [wileyonlinelibrary.com](#)]

constant rate of heating similar to that estimated for the average heating rate of a feed particle in a typical cold cap.^{5,31–33}

Initially, volume changes in melter feed were photographically recorded during heating of loose feed placed in a fused silica crucible.^{5,34,35} One of the drawbacks of this method was feed bridging when a cavity formed below the densified surface of the sample. Because iron-containing waste glass melts are opaque, such a cavity would not be detected, resulting in false data. Another drawback associated with the lack of melt transparency was that the melt stuck to the crucible wall, preventing observation of foam collapsing.

The pellet method avoids these drawbacks. The pellet surfaces are free (thus not confined by walls, except the base) and the sample is observable during the heat treatment including foam collapsing. To make the pellet, the feed had to be compressed. Thus, a precise shape was obtained and good heat conductivity was ensured, which, together with a small sample volume, mostly avoided the problem of temperature gradients in the heated sample.

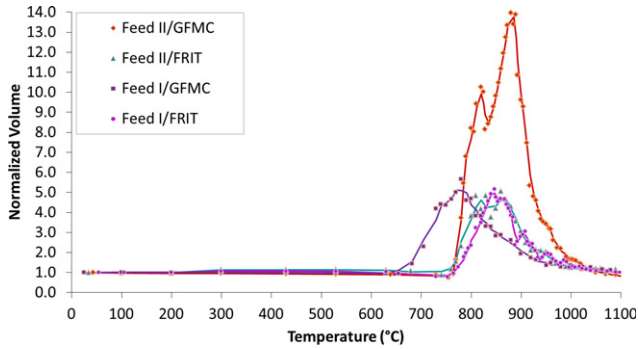


FIGURE 6 Normalized volume of Feed I and Feed II with glass-forming and -modifying chemicals (GFMC) and frit vs temperature: pellets were heated at 10 K/min. [Color figure can be viewed at wileyonlinelibrary.com]

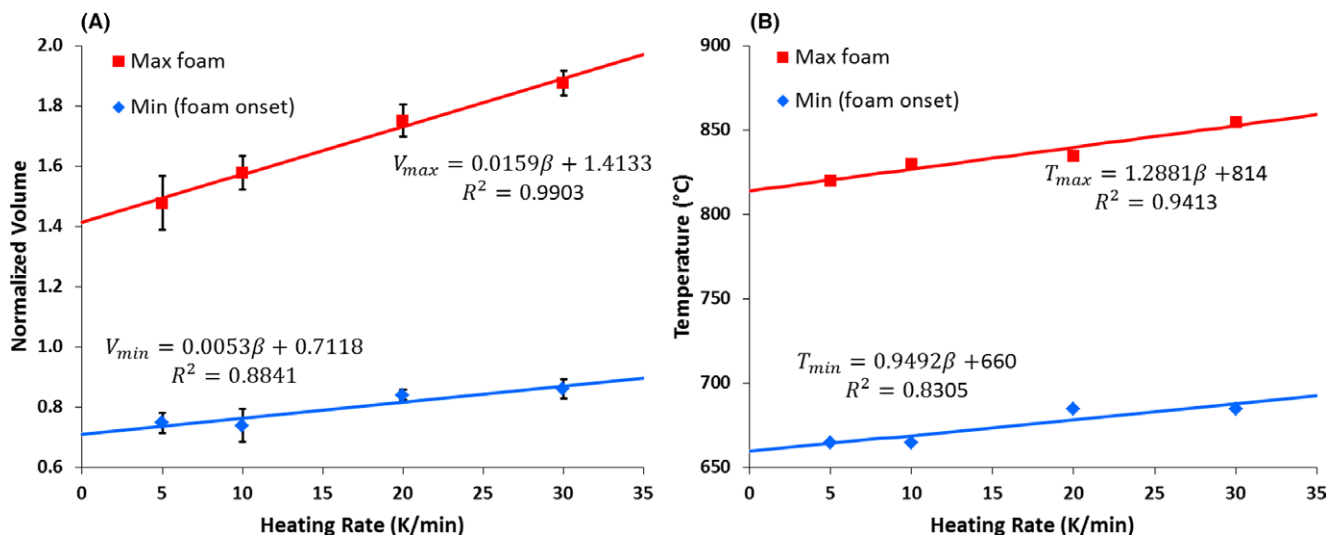


FIGURE 7 Maxima and minima of normalized volume (A) and temperature (B) (A19-original feed with different heating rates, β) based on Figure 3. [Color figure can be viewed at wileyonlinelibrary.com]

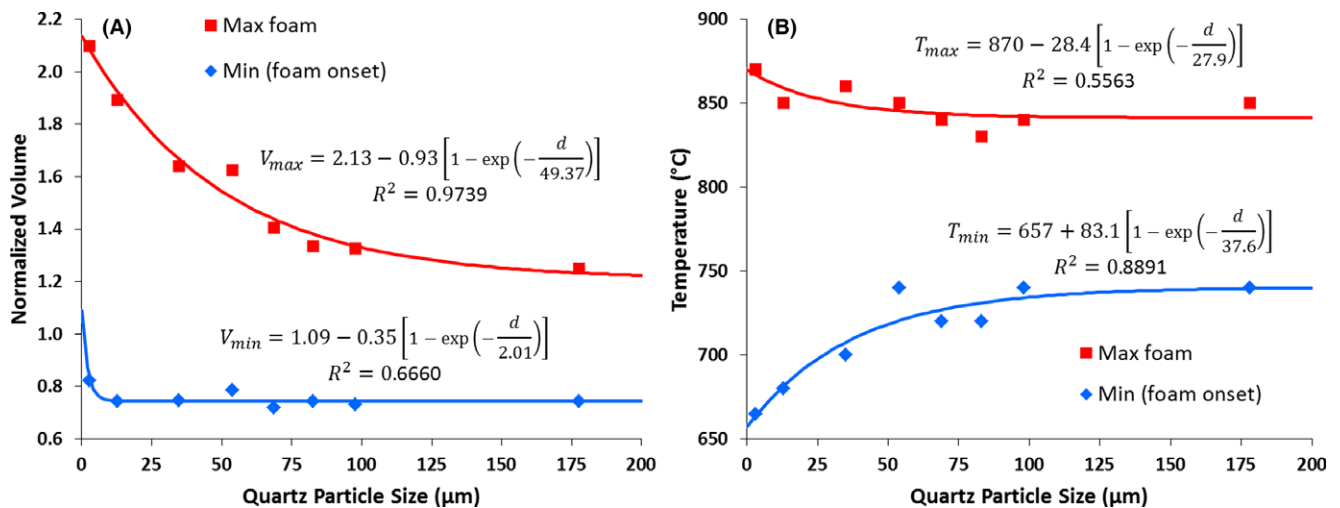


FIGURE 8 Maxima and minima of normalized volume (A) and temperature (B) (A19-original feed with different quartz particle sizes, d) based on Figure 4. [Color figure can be viewed at wileyonlinelibrary.com]

Comparison with the tests that used fused silica crucibles showed that the impact of compression on the volume change was insignificant initially and absent at higher temperatures, at which the initial density was “forgotten.”⁵

The problem of the initial state of the feed is not limited to the compression used to make the pellet. For laboratory studies, the slurry feed is prepared in a way that is similar to the large-scale process, by mixing nonradioactive chemicals with glass-forming and -modifying materials. However, the subsequent treatment is different. In the melter, slurry boils, dries, and is subjected to temperature increase continuously. In the laboratory, slurry is slowly dried and stirred until turned into paste to avoid demixing. The paste is dried, crushed, and then stored for future testing. The

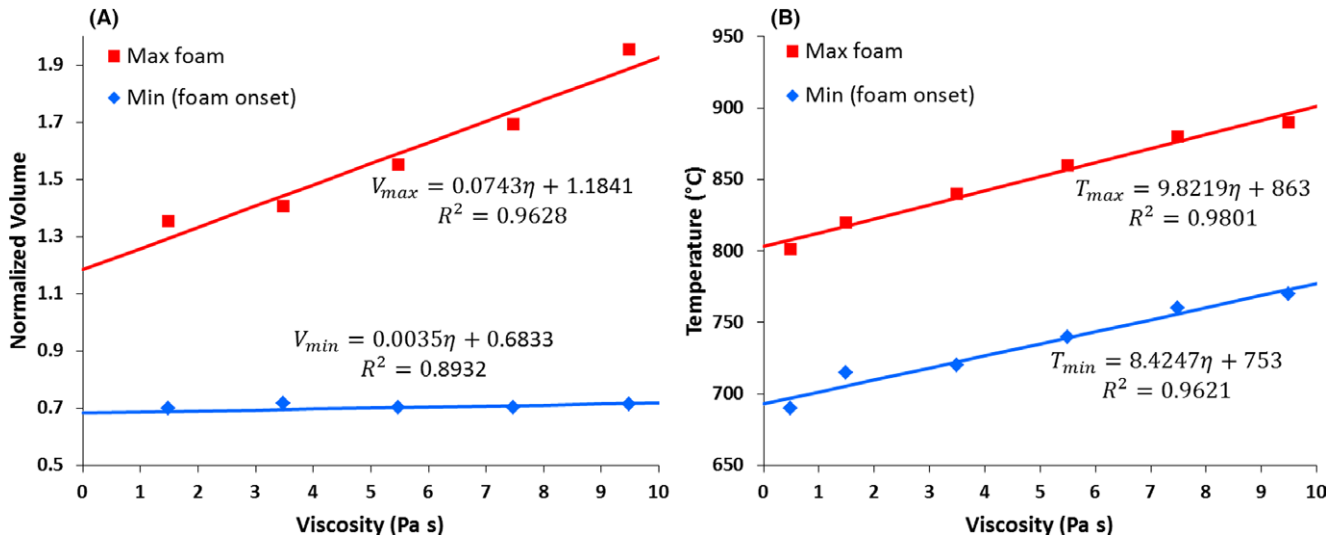


FIGURE 9 Maxima and minima of normalized volume (A) and temperature (B) (A19 feed groups with different viscosities, η) based on Figure 5 [Color figure can be viewed at wileyonlinelibrary.com]

effect of the initial history of feed preparation on later stages of conversion is probably negligible, but the early stages may be affected.

Using a pellet for the feed expansion test is therefore suitable for examining the evolution and collapse of foam, the very last and determining stage of feed-to-glass conversion. In the melter, foam collapses into cavities that are removed by melt currents. The foam collapsing mechanism is different in the pellet, where bubbles coalesce and burst into the atmosphere. Moreover, foam does not collapse fully because secondary bubbles continue to arise from oxygen that evolves from the iron redox reaction as long as the temperature increases.³⁶⁻⁴⁰ In the melter, secondary bubbles ascend from the melt and may accumulate under the cold cap if melt convection is sluggish.¹⁻³ In spite of these differences, pellets provide us important information about the foam layer under the cold cap and essential data for cold cap modeling. To support the pellet experiments, the X-ray tomography⁴¹ of melting pellets is currently being performed, which will give us supplementary information about the conversion process such as the bubble size distribution.

Although foam development is the main focus, the pellet test data are noteworthy for the entire temperature interval from 100°C (typically, the feed had been dried at 105°C) to the cold cap bottom temperature (typically 1100°C). Three stages can be discerned from the volume expansion results. Minor volume expansion occurs at temperatures below ~600°C, within which a large volume of gas is released from batch reactions.⁴²⁻⁴⁶ The gas freely escapes through open porosity,^{3-5,28,46} but its flow is probably hindered in feeds with small densely packed particles, as seen in Figure 4, when small quartz particle size fractions were used. This low-temperature expansion is

occasionally associated with cracking; the cracks are eventually healed.

Pellets shrink as the temperature rises above 600°C, resulting from a sintering-type process in the presence of the liquid phase. This stage lasts for 100°C to 150°C, ending when open pores are gradually sealed by glass-forming melt.

Major volume expansion caused by foaming starts at 700°C-750°C.^{19,31-33} Foam bubbles are generated by the gases evolved from the last residues of feed components, carbonates or nitrates.^{34,35} The earlier the feed pores are sealed by melt, the greater the extent this primary foam reaches before collapsing.

Thus, feed with fine quartz particles generates excessive foam at a lower temperature because rapidly dissolving silica creates a large amount of viscous melt.^{19,22,47}

Feed generates more foam at higher heating rates because the peaks of gas-evolving reactions naturally shift to higher temperatures. On the other hand, a high viscosity of melt stabilizes foam, slowing down the collapse, thus producing more foam that persists to higher temperatures. Accordingly, small quartz particles and high viscosity are likely to decrease the melting rate.^{5,19,22}

Whereas A19 feeds did not exceed $V_{max}=2.2$, the V_{max} of SRNL feeds was ~5 for Feed I with both GFMC and frit and Feed II with frit; for Feed II with GFMC, the V_{max} reached the value of 14. Feed I with GFMC began to foam at a temperature ~60°C lower than any other SRNL feed (Figure 6). This could only happen if enough low-viscosity melt was produced to connect the glass-forming melt and trap evolving gases. Feed II with GFMC released about twice as much CO₂ as Feed I with GFMC,²¹ which could account for the substantially higher extent of foaming of Feed II with GFMC (Figure 6).

A wider temperature interval of foaming indicates a thicker foam layer under the cold cap, whereas larger foam volume suggests a higher porosity of the foam layer.^{21,28} Both thicker foam layer and higher foam porosity are likely to decrease the glass production rate. A narrower foaming interval and smaller foam volume would tend to increase the glass production rate. Feeds made with frit evolve less gas, which is the likely reason that these feeds have significantly narrower temperature intervals of foaming.

5 | CONCLUSIONS

The pellet method was employed to simulate volume changes during the feed-to-glass conversion in the cold cap. The feed pellets were exposed to an increasing temperature until they turned to molten glass. As expected, faster heating intensified foaming and shifted the foaming interval to higher temperatures. Feeds containing fine quartz particles exhibited a massive volume expansion and an early onset of foam resulting from increased viscosity caused by the rapid dissolution of tiny silica particles in the glass-forming melt. For high viscosity melts, foam started at higher temperatures and expanded to larger volumes. Frit reduced feed volume expansion because the pre-melted frit did not contribute to gas evolution. Because of the thermally insulating effect of foam, the width of the foam temperature interval and the porosity of the foam layer affect the rate of melting and thus the waste vitrification efficiency. The data and trends of volume expansion of feeds are indispensable for the development of mathematical modeling of the feed-to-glass conversion in the cold cap.

ACKNOWLEDGMENTS

This work was supported by the U.S. Department of Energy's Waste Treatment & Immobilization Plant Project of the Office of River Protection under the direction of Albert A. Kruger. The Pacific Northwest National Laboratory is operated for the Department of Energy by Battelle Memorial Institute under contract DE-AC05-76RL01830.

REFERENCES

- Krause D, Loch H, *Mathematical Simulation in Glass Technology*. Berlin: Springer; 2012:73–125.
- Hrma P, Kruger AA, Pokorny R. Nuclear waste vitrification efficiency: cold cap reactions. *J Non-Cryst Solids*. 2012;358:3559–3562.
- Pokorny R, Kruger AA, Hrma P. Mathematical modeling of cold cap: effect of bubbling on melting rate. *Ceram Silik*. 2014;58:296–302.
- Pokorny R, Hrma P. Model for the conversion of nuclear waste melter feed to glass. *J Nucl Mater*. 2014;445:190–199.
- Hrma P, Schweiger MJ, Humrickhouse CJ, et al. Effect of glass-batch makeup on the melting process. *Ceramics Silikaty*. 2010;54:193–211.
- Johnson FC, Choi AS, Miller DH, Immel DM, Comparison of HLW glass melting rate between frit and glass forming chemicals using X-Ray computed tomography, SRNL-STI-2014-00562 Revision 0, Aiken, South Carolina, April 2015.
- Vienna JD, Skorski DC, Kim DS, Maty Jás, Glass property models and constraints for estimating the glass to be produced at hanford by implementing current advanced glass formulation efforts, Pacific Northwest National Laboratory, Richland, Washington, EWG-RPT-003, 2013.
- Peeler DK, Lorier TH, Bickford DF, et al. , Melt rate improvement for DWPF MB3: Frit development and model assessment, westinghouse savannah river company, Aiken, South Carolina, WSRC-TR-2001-00131, 2015.
- Miller DH, Smith ME, Lorier TH, The Impact of Frit 202 on Melt Rate for the SB3 Feed System, Savannah River National Laboratory, Aiken, South Carolina, WSRC-TR-2004-00453, 2004.
- Roth G, Weisenburger S. Vitrification of high-level liquid waste: glass chemistry, process chemistry and process technology. *Nucl Engr Design*. 2000;202:197–207.
- Vienna JD. Nuclear waste vitrification in the united states: recent developments and future options. *Inter J Appl Glass Sci*. 2010;1:309–321.
- Gin S, et al. An international initiative on long-term behavior of high-level nuclear waste glass. *Mater Today*. 2013;16:243–248.
- Jacoutot L, Brun P, Gagnoud A, Fautrelle Y. Numerical modelling of natural convection in molten glass heated by induction. *Chem Engr Process*. 2008;47:449–455.
- Kawamura T, Ito K, Sakai T, Nakajima M, Fujiwara K, Ohshima H. Numerical analysis of platinum group particle behavior in vitrification melter. *Atom Energy Soc Jpn*. 2008;7:297–307.
- Pokorny R, Hilliard ZJ, Dixon DR, et al. One-dimensional cold cap model for melters with bubblers. *J Am Ceram Soc*. 2015;98:3112–3118.
- Kuhn WS. Mathematical modeling of batch melting in glass tanks. In: Krause D, Loch H, eds. *Mathematical Simulation in Glass Technology*. Berlin: Springer; 2002:73–110.
- Choudhary MK. Recent advances in mathematical modeling of flow and heat transfer phenomena in glass furnaces. *J Am Ceram Soc*. 2002;85:1030–1036.
- Hrma P, Vienna JD, Piepel GF, LoPresti CA, Schweiger MJ. Property composition relationships for hanford high-level waste glasses melting at 1150°C. Richland, Washington: Pacific Northwest National Laboratory, PNL-10359, Vol. 1 and 2, 1994.
- Lee S, Hilliard Z, Heilman-Moore J. S., et al. , The Effect of quartz particle size and melt viscosity on HLW melter feed using pellet test response; presented at the WM2016 Conference, Phoenix, Arizona, March 6-10, 2016.
- Matlack KS, Gan H, Chaudhuri M, et al. , DM100 and DM1200 melter testing with high waste loading glass formulations for hanford high-aluminum HLW streams. Washington, DC: Vitreous State Laboratory and Columbia, Maryland: EnergySolutions, VSL-10R1690-1, 2010.
- VanderVeer B, Hrma P, Hilliard Z, Peeler MD, Schweiger MJ, Comparison of high level waste glass feeds containing frit and

- glass forming chemicals, presented at the WM2016 Conference. Phoenix, Arizona, March 6-10, 2016.
22. Schweiger MJ, Hrma P, Humrickhouse CJ, Marcial J, Riley BJ, TeGrotenhuis NE. Cluster formation of silica particles in glass batches during melting. *J Non-Cryst Solids*. 2010;356:1359–1367.
 23. Hrma P, Han S. Effect of glass composition on activation energy of viscosity in glass-melting-temperature range. *J Non-Cryst Solids*. 2012;358:1818–1829.
 24. Hrma P, Arrigoni BM, Schweiger MJ. Viscosity of many-component glasses. *J Non-Cryst Solids*. 2009;355:891–902.
 25. Hrma P, Kruger AA. High-temperature viscosity of many-component glass melts. *J Non-Cryst Solids*. 2016;437:17–25.
 26. Hrma P. Arrhenius model for high-temperature glass viscosity with a constant pre-exponential factor. *J Non-Cryst Solids*. 2008;354:1962–1968.
 27. Hrma P, Arrigoni BM, Schweiger MJ. Glass viscosity as a function of temperature and composition: a model based on adam-gibbs equation. *J Non-Cryst Solids*. 2008;354:3389–3399.
 28. Hilliard Z, Hrma P. A method for determining bulk density, material density, and porosity of melter feed during nuclear waste vitrification. *J Am Ceram Soc*. 2016;99:98–105.
 29. Raether F, Krauss M. In situ measurements of batch glass during melting. *Glass Sci Technol*. 2004;77:118–123.
 30. Pokorny R, Pierce DA, Hrma P. Kinetics of batch melting reactions. *Thermochim Acta*. 2012;541:8–14.
 31. Henager SH, Hrma P, Swearingen KJ, Schweiger MJ, Marcial J, TeGrotenhuis NE. Conversion of batch to molten glass, I: volume expansion. *J Non-Cryst Solids*. 2011;357:829–835.
 32. Hrma P, Marcial J, Swearingen KJ, Henager SH, Schweiger MJ, TeGrotenhuis NE. Conversion of batch to molten glass, II: dissolution of quartz particles. *J Non-Cryst Solids*. 2011;357:820–828.
 33. Hrma P, Marcial J. Dissolution retardation of solid silica during glass-batch melting. *J Non-Cryst Solids*. 2011;357:2954–2959.
 34. Hrma P, Maty Jás, Kim D. The chemistry and physics of melter cold cap, 9th Biennial Int. Conf. on Nucl. And Hazardous Waste Management, Spectrum '02, American Nuclear Society, CD-ROM, 2002.
 35. Darab JG, Meiers EM, Smith PA. Behavior of simulated hanford slurries during conversion to glass. *Mat Res Soc Proc*. 1999;556:215–222.
 36. Petersen RR, König J, Yue Y. The mechanism of foaming and thermal conductivity of glasses foamed with MnO_2 . *J Non-Cryst Solids*. 2015;425:74–82.
 37. Beerkens R, Laimböck P. Foaming of glass melts. *Ceram Eng Sci Proc*. 2008;21:41–58.
 38. Petersen RR, König J, Yue Y. In situ evaluation of foaming ability of glass melts using heating microscope. *Inter J Appl Glass Sci*. 2016. doi: 10.1111/ijag.12189.
 39. Fedorov AG, Pilon L. Glass foams: formation, transport, properties, and heat, mass, and radiation transfer. *J Non-Cryst Solids*. 2002;311:154–173.
 40. Hrma P. Melting of foaming batches: nuclear waste glass. *Glasstech Ber*. 1990;63:360–369.
 41. Watanabe K, Yano T, Takeshita K, Minami K, Ochi E. X-Ray CT imaging of vitrified glasses containing stimulant radioactive wastes: structure and chemical reactions of glass beads and wastes in the cold cap. *Glass Technol Eur J Glass Sci Technol A*. 2012;53:273–278.
 42. Marcial J, Chun J, Hrma P, Schweiger MJ. Effect of bubbles and silica dissolution on melter feed rheology during conversion to glass. *Environ Sci Technol*. 2014;48:12173–12180.
 43. Chun J, Pierce DA, Pokorny R, Hrma P. Cold-cap reactions in vitrification of nuclear waste glass: experiments and modeling. *Thermochim Acta*. 2013;559:32–39.
 44. Kissinger HE. Reaction kinetics in differential thermal analysis. *Anal Chem*. 1957;29:1702–1706.
 45. Rodriguez CP, Chun J, Schweiger MJ, Kruger AA. Application of evolved gas analysis to cold-cap reactions of melter feeds for nuclear waste vitrification. *Thermochim Acta*. 2013;592:86–92.
 46. Xu K, Hrma P, Rice JA, Schweiger MJ, Kruger AA. Conversion of nuclear waste to molten glass: cold-cap reactions in crucible test. *J Am Ceram Soc*. 2016;99:2964–2970.
 47. Pokorny R, Hrma P. Mathematical modeling of cold cap. *J Nucl Mater*. 2012;429:245–256.

How to cite this article: Lee SM, VanderVeer BJ, Hrma P, et al. Effects of heating rate, quartz particle size, viscosity, and form of glass additives on high-level waste melter feed volume expansion. *J Am Ceram Soc*. 2017;100:583–591.